Supporting Information

Diiron Dithiolate Complex-Induced Helical Structure of Histone and Application in Photochemical Hydrogen Generation

Xiantao Hu, Weijian Chen, Shuyi Li, Jian Sun, Ke Du, Qiuyu Xia and Fude Feng*

Key Laboratory of High Performance Polymer Material and Technology of Ministry of Education, Department of Polymer Science & Engineering, School of Chemistry & Chemical Engineering, Nanjing University, Nanjing 210023, China.

*Corresponding author: fengfd@nju.edu.cn

Contents

Figure S1	S-3
Figure S2	S-3
Figure S3	S-3
Figure S4	S-4
Figure S5	S-4
Figure S6	S-5
Figure S7	S-5
Table S1	S-6
References	S-7

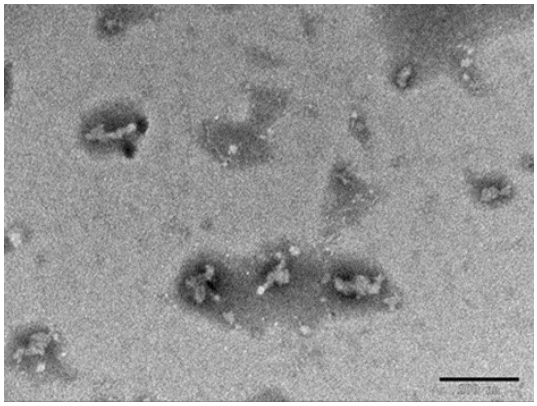

Figure S1. TEM image of histone H1 (1 mg mL^{-1}). Scale bar, 200 nm.

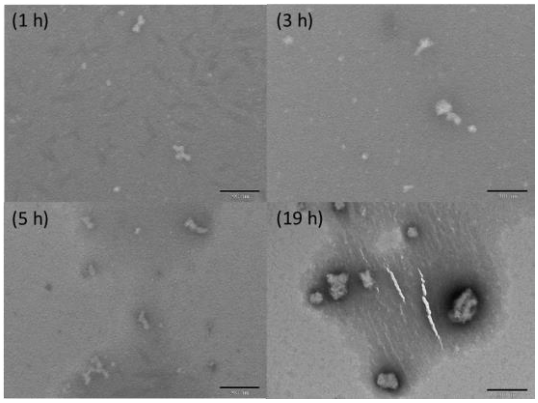

Figure S2. TEM images of H-Fe-1 after varying reaction time. Scale bar, 200 nm.

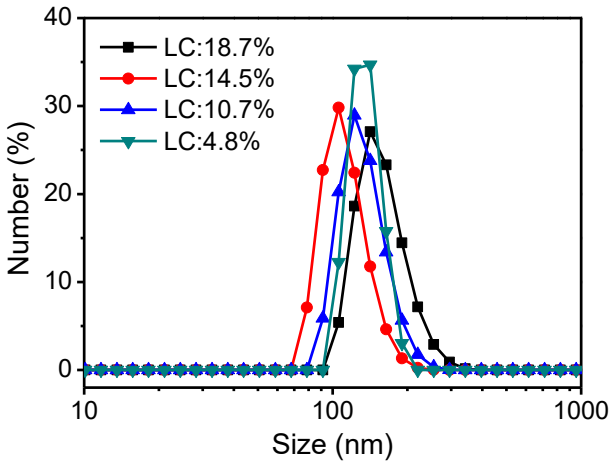

Figure S3. DLS analysis of H-Fe nanoparticles with varied LC in water (pH 5.0).

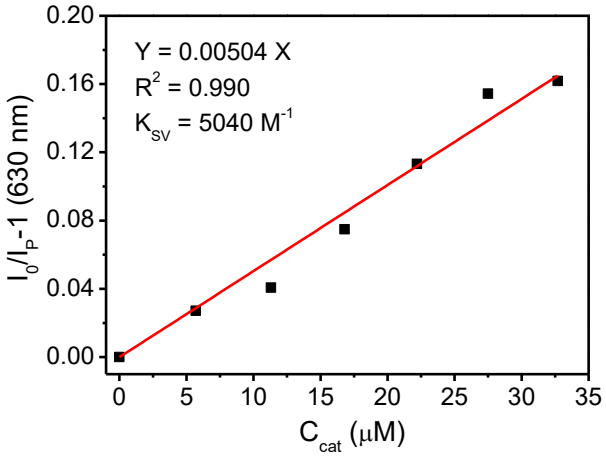

Figure S4. The Stern-Volmer plots of (I_0/I_p-1) values as a function of C_{cat} by successive addition of H-Fe-1 into a solution of $Ru(bpy)_3Cl_2$ (5 μM) and sodium ascorbate (10 mM). $Ru(bpy)_3^{2+}$ was excited at 456 nm and luminesced at 630 nm.

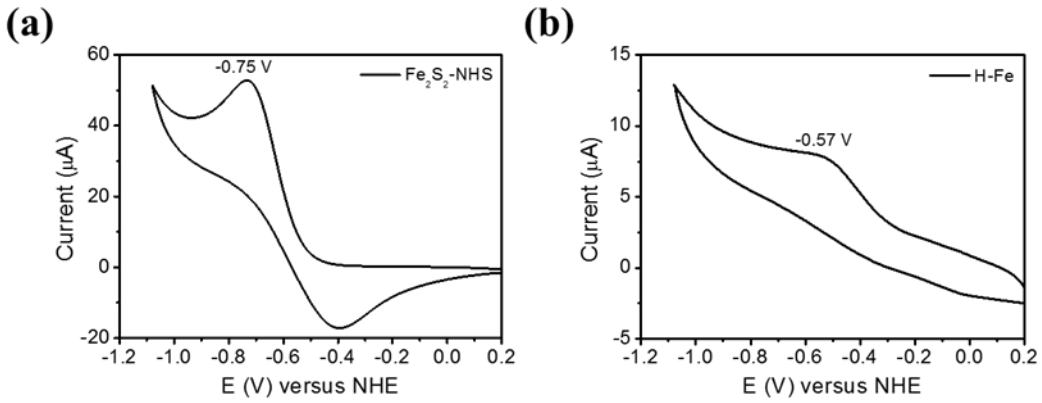

Figure S5. Cyclic voltammograms of (a) Fe_2S_2-NHS (45 μM) in CH_3CN in the presence of 0.1 M (n-Bu_4N)PF_6 and (b) H-Fe-1 (45 μM incorporated catalyst) in 0.1 M aq. Na_2SO_4 solution. Scan rate, 50 mV s^{-1}.

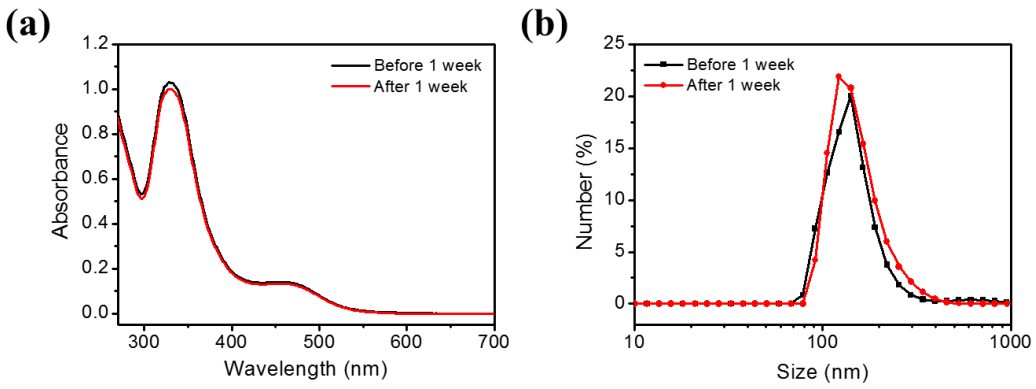

Figure S6. The UV-vis absorption spectra (a) and DLS analysis (b) of H-Fe-1 (120 μM incorporated catalyst) before and after 1-week storage protected from light at 4 °C.

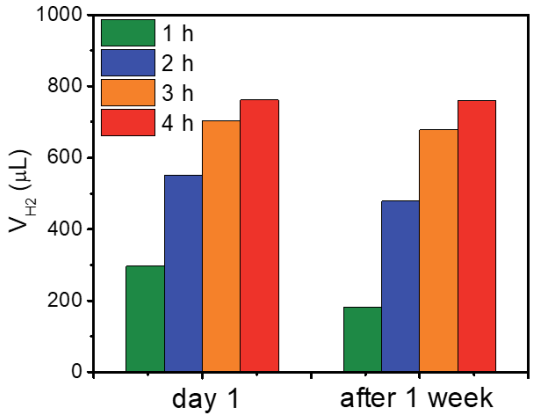

Figure S7. Photocatalytic H_2 production from H-Fe-1 before and after 1-week storage at 4 °C. The reaction mixture (pH 5.0) contained incorporated catalyst (4 μM), $Ru(bpy)_3^{2+}$ (400 μM), and ascorbic acid (160 mM).

Table S1. Comparison of reported photochemical systems based on peptides and proteins

Protein	PS	Catalyst	Electron donor	Light Source	TON[a]	Enhan-cement	TOF[a]	Time	Ref.
Flavodoxin	[Ru(4-CH_2Br-4'-bpy)(bpy)$_2$]·2PF_6 (5 μM)	NiC([Ni-($P_2^{Ph}N_2^{Ph}$)$_2$] (BF_4)$_2$) (5 μM)	Sodium ascorbate (0.1 M)	λ > 375 nm	620 ± 80	N.A.	410 ± 30 h^{-1} or ~6.8 min^{-1}	N.A.	1
Cytochrome b_{562}	$Ru(bpy)_3^{2+}$ (1 mM)	CoPP(IX) (10.8 μM)	Sodium ascorbate (0.1 M)	110 mW cm^{-2}, λ > 410 nm	310	~ 2.5	N.A.	8 h	2
Ferredoxin	[Ru(4-CH_2Br-4'-bpy) (bpy)$_2$]·2PF_6	[Co(dmgH)$_2$ pyridyl]Cl	Sodium ascorbate (0.1 M)	λ > 375 nm	650 ± 150 (PS-based) or ~271	N.A.	170 ± 10 h^{-1} (PS-based) or 1.2 min^{-1}	N.A.	3
Ferredoxin	[Ru(4-CH_2Br-4'-CH_3-2,2'-bpy) (bpy)$_2$]·2PF_6	Co(dmgBF_2)$_2$·2H_2O	Sodium ascorbate (0.1 M)	λ > 375 nm	210 ± 60 (PS-based) or ~76	N.A.	50 ± 10 h^{-1} (PS-based) or 0.3 min^{-1}	8 h	4
Nitrobindin	$Ru(bpy)_3^{2+}$ (140 μM)	(μ-S-Cys)$_2$ $Fe_2(CO)_6$ core (7.8 μM)	Sodium ascorbate (0.1 M)	λ > 410 nm	130	~ 1	2.3 min^{-1}	3 h	5
Myoglobin	$Ru(bpy)_3^{2+}$ (1 mM)	CoPP(IX) (5 μM)	Sodium ascorbate (0.1 M)	110 mW cm^{-2}, λ > 400 nm	518	4.32	1.47 min^{-1}	8 h	6
Flavodoxin	PSI monomer (80 nM)	[Ni($P_2^{Ph}N_2^{Ph}$)$_2$] (BF_4)$_2$ 2.4 uM	Sodium ascorbate (0.1 M)	λ > 400 nm	2825 (PS-based)	2	1.25 s^{-1} (PS-based)	4 h	7
Aβ_{16-22} peptide	Eosin Y	Pt (10 wt%)	TEOA (10 vol%)	λ > 420 nm	92.9	5	0.39 min^{-1}	20 h	8
Cytochrome c_{556}	[Ru(tpy)(bpy)(im)](PF_6)$_2$ (140 μM)	[FeFe]Pep-18 (H10A) (140 μM)	Sodium ascorbate (0.1 M)	λ > 410 nm	9	N.A.	0.19 min^{-1}	3 h	9
Helical peptide	$Ru(bpy)_3^{2+}$ (150 μM)	(μ-S-$(CH_2)_3$-S) [$Fe_2(CO)_6$] (9.33 μM)	Sodium ascorbate (0.1 M)	110 mW cm^{-2}, λ > 410 nm	84	N.A.	N.A.	2.3 h	10
Cytochrome *c*	$Ru(bpy)_3^{2+}$ (140 μM)	(μ-S-Cys)$_2$ [$Fe_2(CO)_6$] (14 μM)	Sodium ascorbate (0.1 M)	189 mW cm^{-2}, λ > 410 nm	82	6.83	0.21 min^{-1}	3 h	11
Apoferritin	$Ru(bpy)_3^{2+}$ (1 mM)	FeFe–COOH (51 μM)	Ascorbic acid (0.05 M)	200 mW cm^{-2}, λ > 400 nm	31 or 1.58 (PS-based)	8.5	N.A.	3 h	12
Histone H1	$Ru(bpy)_3^{2+}$ (400 μM)	Fe_2S_2-lip (4 μM)	Ascorbic acid (0.16 M)	200 mW cm^{-2}, λ > 400 nm	359 Or 3.59 (PS-based)	6	1.8 min^{-1}	6 h	This work

[a] TON and TOF were calculated based on the amount of catalyst unless otherwise stated.

References

(1) Soltau, S. R.; Niklas, J.; Dahlberg, P. D.; Mulfort, K. L.; Poluektov, O. G.; Utschig, L. M. Charge Separation Related to Photocatalytic H_2 Production from a Ru−Apoflavodoxin−Ni Biohybrid. *ACS Energy Lett.* **2017**, 2, 230-237.

(2) Sommer, D. J.; Vaughn, M. D.; Clark, B. C.; Tomlin, J.; Roy, A.; Ghirlanda, G. Reengineering cyt b_{562} for Hydrogen Production: A facile Route to Artificial Hydrogenases. *Biochim. Biophys. Acta* **2016**, 1857, 598-603.

(3) Soltau, S. R.; Dahlberg, P. D.; Niklas, J.; Poluektov, O. G.; Mulfort, K. L.; Utschig, L. M. Ru-Protein-Co Biohybrids Designed for Solar Hhydrogen Production: Understanding Electron Transfer Pathways Related to Photocatalytic Function. *Chem. Sci.* **2016**, 7, 7068-7078.

(4) Soltau, S. R.; Niklas, J.; Dahlberg, P. D.; Poluektov, O. G.; Tiede, D. M.; Mulfort, K. L.; Utschig, L. M. Aqueous Light Driven Hydrogen Production by a Ru-ferredoxin-Co Biohybrid. *Chem. Commun.* **2015**, 51, 10628-10631.

(5) Onoda, A.; Kihara, Y.; Fukumoto, K.; Sano, Y.; Hayashi, T. Photoinduced Hydrogen Evolution Catalyzed by a Synthetic Diiron Dithiolate Complex Embedded within a Protein Matrix. *ACS Catal.* **2014**, 4, 2645-2648.

(6) Sommer, D. J.; Vaughn, M. D.; Ghirlanda, G. Protein Secondary-shell Interactions Enhance the Photoinduced Hydrogen Production of Cobalt Protoporphyrin IX. *Chem. Commun.* **2014**, 50, 15852-15855.

(7) Silver, S. C.; Niklas, J.; Du, P. W.; Poluektov, O. G.; Tiede, D. M.; Utschig, L. M. Protein Delivery of a Ni Catalyst to Photosystem I for Light-Driven Hydrogen Production. *J. Am. Chem. Soc.* **2013**, 135, 13246-13249.

(8) Pan, Y. X.; Cong, H. P.; Men, Y. L.; Xin, S.; Sun, Z. Q.; Liu, C. J.; Yu, S. H. Peptide Self-Assembled Biofilm with Unique Electron Transfer Flexibility for Highly Efficient Visible-Light-Driven Photocatalysis. *ACS Nano* **2015**, 9, 11258-11265.

(9) Sano, Y.; Onoda, A.; Hayashi, T. Photocatalytic Hydrogen Evolution by a Diiron Hydrogenase Model based on a Peptide Fragment of Cytochrome c_{556} with an Attached Diiron Carbonyl Cluster and an Attached Ruthenium Photosensitizer. *J. Inorg. Biochem.* **2012**, 108, 159-162.

(10) Roy, A.; Madden, C.; Ghirlanda, G. Photo-induced Hydrogen Production in a Helical Peptide

Incorporating a [FeFe] Hydrogenase Active Site Mimic. *Chem. Commun.* **2012**, 48, 9816-9818.

(11) Sano, Y.; Onoda, A.; Hayashi, T. A Hydrogenase Model System based on the Sequence of Cytochrome *c*: Photochemical Hydrogen Evolution in Aqueous Media. *Chem. Commun.* **2011**, 47, 8229-8231.

(12) Chen, W. J.; Li, S. Y. ; Li, X.; Zhang, C.; Hu, X. T.; Zhu, F.; Shen, G. S.; Feng, F. D. Iron Sulfur Clusters in Protein Nanocages for Photocatalytic Hydrogen Generation in Acidic Aqueous Solutions. *Chem. Sci.* **2019**, 10, 2179-2185.